

## CFD ANALYSIS OF A V-RIB WITH GAP ROUGHENED SOLAR AIR HEATER

Jitesh RANA<sup>a</sup>, Anshuman SILORI<sup>a</sup>, Rajesh MAITHANI<sup>a\*</sup>, Sunil CHAMOLI<sup>a</sup>

<sup>a</sup>Department of Mechanical Engineering, DIT University, Dehradun, India.

\*Corrospounding author; Email: rajeshmaithani1@gmail.com

*A computational fluid dynamics (CFD) analysis of a solar air heater has been carried out using v-shaped ribs as artificial roughness on the absorber plate. The relative roughness pitch ( $P/e=6-12$ ), Reynolds number ( $Re=3800-18000$ ), and relative roughness height ( $e/D=0.042$ ), angle of attack ( $\alpha=30^\circ-75^\circ$ ) have been selected as design variables of V-shaped rib for analysis. ANSYS FLUENT 15.0 with renormalization group  $k-\varepsilon$  turbulence model is selected for the analysis of computational domain of solar air heater. The enhancement of Nusselt number and friction factor with Reynolds number for different values of a relative roughness pitch ( $P/e$ ) are presented and discussed by CFD analysis. The effect of angle of attack ( $\alpha$ ) and Reynolds number on enhancement of Nusselt number ( $Nu$ ) and friction factor ( $f$ ) is also presented. The optimum value of rib configuration based on constant pumping power requirement has been derived using thermo-hydraulic performance parameter and has been found maximum at angle of attack of  $60^\circ$  and  $P/e = 10$ .*

Keywords: *Nusselt Number, Friction Factor, CFD, V-ribs*

### 1. Introduction

The use of artificial roughness is an effective method to augment the heat transfer rate in a solar air heater duct. The artificial roughness enhances the heat transfer rate by creating turbulence but in turn imposes a pressure drop penalty. The roughness on the absorber plate can be produced in many ways on the surface by attaching the ribs, baffles, winglets, blockages etc. The arrangements of turbulence promoters on the absorber plate are done in various orientation and configuration. Researchers have investigated the effect of using artificial roughness on heat transfer and friction factor using different type of turbulent promoters on the underside of the absorber plate. Singh et al. [1] investigated experimentally the heat transfer characteristics of rectangular duct having its one broad wall heated and roughened with periodic 'discrete V-down rib. Kumar and Saini [2] used arc shaped geometry in order to find out the fluid flow and heat transfer characteristics of solar air heater using CFD. Chaube et al. [3] used artificial roughness in the form of ribs and performed a computational analysis of heat transfer augmentation and flow characteristics in channel flow arrangements. Yadav and Bhagoria [4] by CFD analysis investigated the performance of solar air heater having circular transverse rib as a roughness. Varun et al. [5] carried out an experimental work using a combination of inclined and transverse ribs in order to determine the heat transfer and friction characteristics. The study revealed that the best thermal performance was obtained for relative roughness pitch value of 8 and relative roughness height value of 0.030. Tanda [6]

carried out an experimental study in a rectangular channel having one wall roughened with angled continuous ribs, transverse continuous and broken ribs, and discrete V-shaped ribs to investigate the heat transfer and friction characteristics. Muluwork [7] carried out an experimental analysis using artificial roughness provided in the form of V-shaped staggered discrete ribs and reported that at an angle of attack of  $60^\circ$  provide the maximum heat transfer enhancement. Momin et al. [8] studied the effect of V-shaped rib geometry on heat transfer and fluid flow characteristics with absorber plate roughened with V-shaped ribs on its underside. Kumar et.al. [9] studied artificial roughness in the form of circular wire in discrete angled rib arrangement using Computational Fluid Dynamics. The effect of roughness geometry on heat transfer and friction factor and performance enhancement was investigated for roughness parameters,  $P/e=8$ ,  $e/D=0.043$ ,  $d/W=0.25$ ,  $g/e=1.0$ ,  $\alpha=60^\circ$ . Kumar et.al. [10] analyzed discrete multi V-rib with staggered rib shape on the average Nusselt number, average friction factor and overall thermal performance using the RNG  $k-\varepsilon$  turbulent model. The investigation reveals that the overall thermal performance of discrete multi V-rib with staggered rib is 6% higher as relative to other rib shapes. Sahu and Bhagoria [11] carried out an experimental investigation using  $90^\circ$  broken ribs as roughness elements to study the thermal performance of a solar air heater channel flow and reported that at the pitch of 20mm maximum enhancement in heat transfer occurred, while the efficiency lies in the range of 51–83.5%. Sharma and Thakur [12] carried a CFD analysis for V-shaped rib roughness attached on the absorber plate at an angle of attack of  $60^\circ$  to determine the heat transfer and friction loss characteristics of a solar air heater. Maithani & Saini [13] experimentally investigated the heat transfer and friction characteristics of V-shaped ribs with symmetrical gaps roughened solar air heater duct. They reported the enhancement in the Nusselt number and friction factor of the order of 3.67 and 3.66, respectively. In the present study a CFD analysis of an artificially roughened solar air heater has been carried out in order to determine the heat transfer and friction factor characteristics of V-shaped ribs with gaps on each limb is used roughness.

## **2.Details of the solar air heater duct**

The three dimensional computational domain of the solar air heater has been generated in design modeler of ANSYS 15.0. The diameter of rib considered is 2mm. The flow system is a rectangular duct with test, entry and exit sections. The length, entry section and exit section of the solar air heater duct are 1100, 300 and 300mm, respectively. The width (W) and height (H) of the duct are 300 and 25mm, respectively. The artificial roughness on the absorber plate is in the form of V-rib with symmetrical gaps for analysis. The CFD investigation is carried out using fixed relative roughness height ( $e/D$ ) of 0.042, relative roughness pitch ( $P/e$ ) in the range of 6-12, and Reynolds number varying from 3000-18000. A uniform heat flux of  $1000 \text{ W/m}^2$  is set on the top surface of the computational domain. The geometrical and operating parameters used for analysis are listed in tables 1. The schematic view of roughness geometry is shown in fig.1.

**Table.1.Geometrical parameters of duct used in ANSYS FLUENT 15.0.**

<b>Geometrical Parameters</b>	<b>Values</b>
Length (L)	1100mm
Width (W)	300mm
Height (H)	25mm
Number of gaps ( $N_g$ )	4
Gap size (g)	4mm
Angle of attack ( $\alpha$ )	30°-75°
relative roughness pitch (P/e)	6-12

### 3. Computational fluid dynamics

#### 3.1 Fluid domain formations in ANSYS fluent

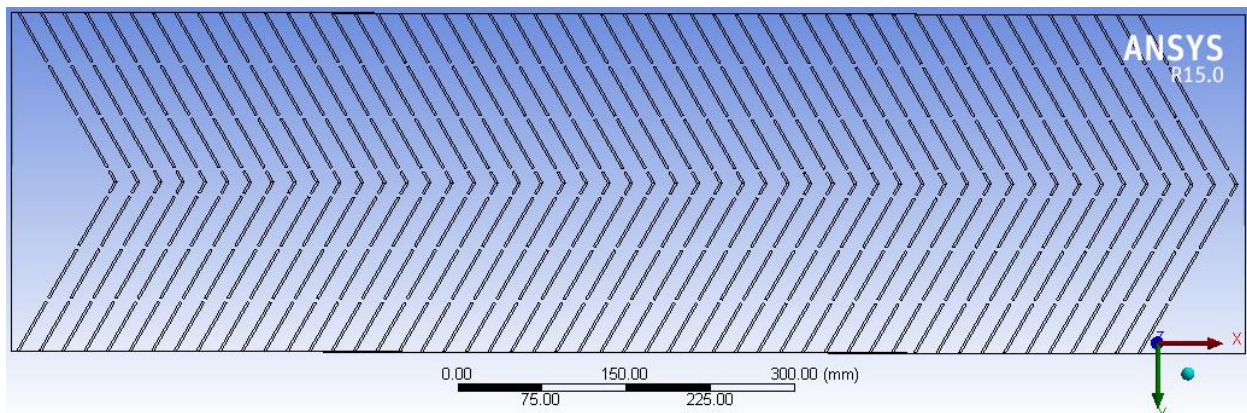


**Fig.1.Duct in ANSYS fluent 15.0**

#### 3.2. Mesh formation

In order to critically examine the study of stream and heat transfer in the inter-rib regions fine meshing (triangular mesh) is done in the rib region while in other regions coarser mesh has been used as shown in fig 3. The mesh are correctly generated in order to capture the boundary layer properly. Mesh independence tests were carried out in five steps with various numbers of cells (1657834, 1775885, 1986456, 2121789 and 2375325) and it was observed that as a number of grids increase average Nusselt number also increases up to 2375325 cells, further increase in cells has negligible variation in average Nusselt number. The grid with 2375325 cells is used for all analysis.

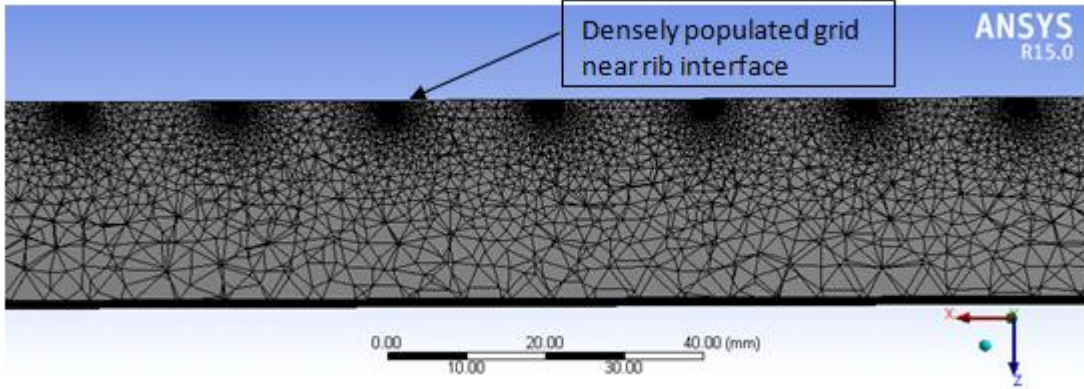


**Fig.2. Rectangular duct section with unstructured mesh**

### 3.3 Governing equations

In the present study a three-dimensional CFD simulation by ANSYS FLUENT to determine the heat transfer and flow friction was conducted. The CFD simulation involves mathematical solutions of the conservation equations for mass, momentum, and energy. In the cartesian tensor system, these governing equations can be written as

**Continuity equation:**

$$\frac{\partial}{\partial x_i}(\rho u_i) = 0 \quad (1)$$

**Momentum equation:**

$$\frac{\partial}{\partial x_i}(\rho u_j u_j) = -\frac{\partial p}{\partial x_i} + \frac{\partial}{\partial x_j} \left[ \mu \left( \frac{\partial u_i}{\partial x_j} + \frac{\partial u_j}{\partial x_i} \right) \right] + \frac{\partial}{\partial x_j} (-\overline{\rho u'_i u'_j}) \quad (2)$$

**Energy**

$$\frac{\partial}{\partial x_i}(\rho u_j T) = \frac{\partial}{\partial x_j} \left( (\Gamma + \Gamma_t) \frac{\partial T}{\partial x_j} \right) \quad (3)$$

Where  $\Gamma$  and  $\Gamma_t$  are molecular thermal diffusivity and turbulent thermal diffusivity, respectively.

### 3.4. Solution method

The CFD analysis of solar air heater duct with V-ribs with symmetrical gap shaped artificial roughness is carried out. The flow equations are solved using RNG k- $\epsilon$  turbulence model as it shows very good agreement with the empirical relations. A second order scheme is selected for energy and momentum equations. The convergence criteria of  $10^{-3}$  for the residuals of continuity equations,  $10^{-6}$  for the residuals of velocity components and  $10^{-6}$  for the residuals of energy. The conservation equations are solved iteratively until convergence.

### 3.5. Selection and validation of the model

The selection of turbulence model is carried out by many researchers viz. Yadav and Bhagoria[14], Kumar and Saini[15]. They compared the Nusselt number predicted by different turbulence models (Standard k-ε model, Standard k-ω, Shear stress transport k-ω model, RNG k-ε turbulence model and Realizable k-ε model) with Dittus-Boelter correlation. The result reveals that RNG k-ε turbulence model was in good agreement with Nusselt number predicted by Dittus-Boelter correlation. Hence the current study has been carried out using RNG k-ε turbulence model.

The Nusselt number for a smooth rectangular duct is given by the Dittus-Boelter equation as;

$$Nu_s = 0.023 Re^{0.8} Pr^{0.4} \quad (4)$$

The friction factor for a smooth rectangular duct is given by the modified Blasius equation as;

$$f = 0.085 Re^{-0.25} \quad (5)$$

The comparison of CFD and theoretical results are depicted in Fig.4.

The efficiency of any solar heater is determined by two parameters i.e. Thermal performance and hydraulic performance. The Nusselt number (Nu) and friction factor (f) in CFD analysis were calculated using the following relations,

$$Nu = \frac{hD}{k} \quad (6)$$

$$f = \frac{2\Delta PD}{\rho U^2 L} \quad (7)$$

The thermo hydraulic performance value greater than unity depicts it is advantageous to use roughened duct as compared to smooth duct. The thermo hydraulic performance of the artificial roughness was calculated using the following relation:

$$\eta = \frac{Nu/Nu_s}{(f/f_s)^{1/3}} \quad (8)$$

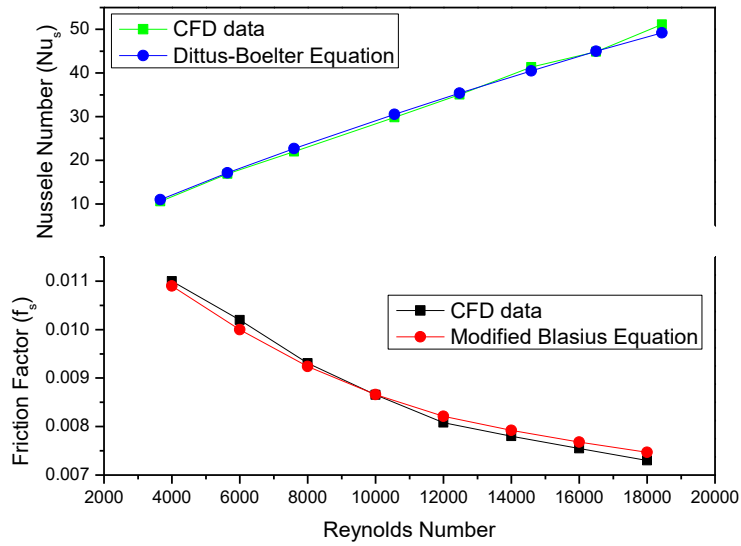


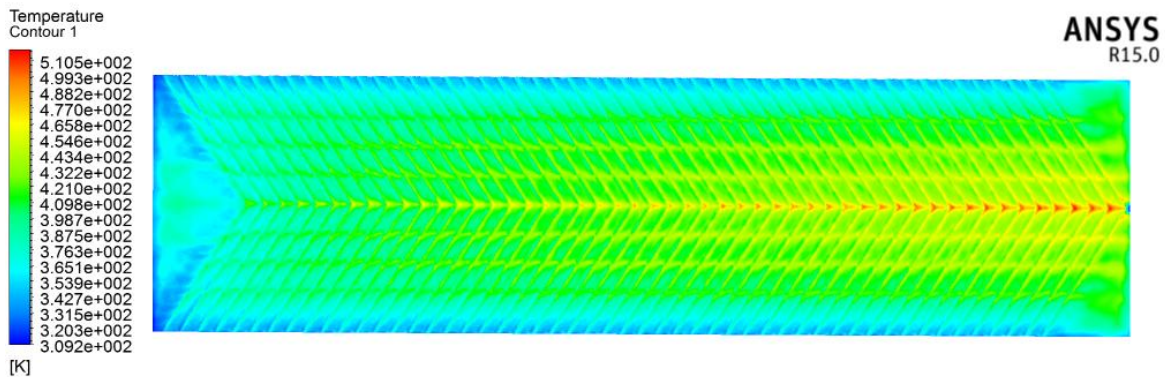
Fig. 4. Comparison of CFD data with Dittus Boelter and Blasius equation for the smooth duct.

#### 4. Results and discussion

The effects of various flow and roughness parameters on the heat transfer and friction characteristics of flow of air in a roughened Rectangular duct are presented below.

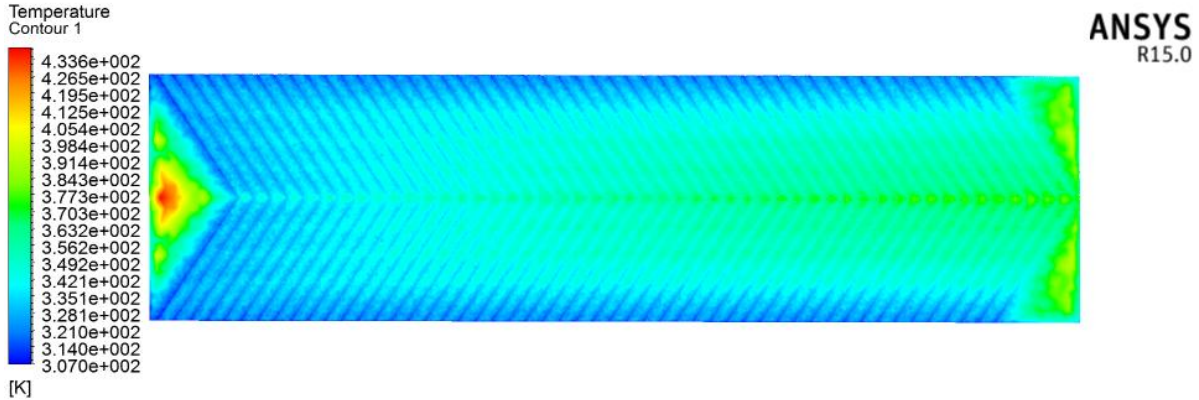
##### 4.1. Temperature and velocity profile

The temperature contours of the absorber plate are shown in fig.4. For different values of Reynolds number. It can be seen that as the Reynolds number increases the turbulent intensity increases which increase the heat transfer rate and thus have a low surface temperature. The hot zone also reduced with an increase in Reynolds number. fig.5. Shows the variation of pressure across the duct at Reynolds Number of 15000. It is observed that the pressure is maximum at inlet section and it further decreases throughout the duct.





(a)



(b)

Fig.4. Temperature contour at Reynolds number (a) 3000 (b) 15000

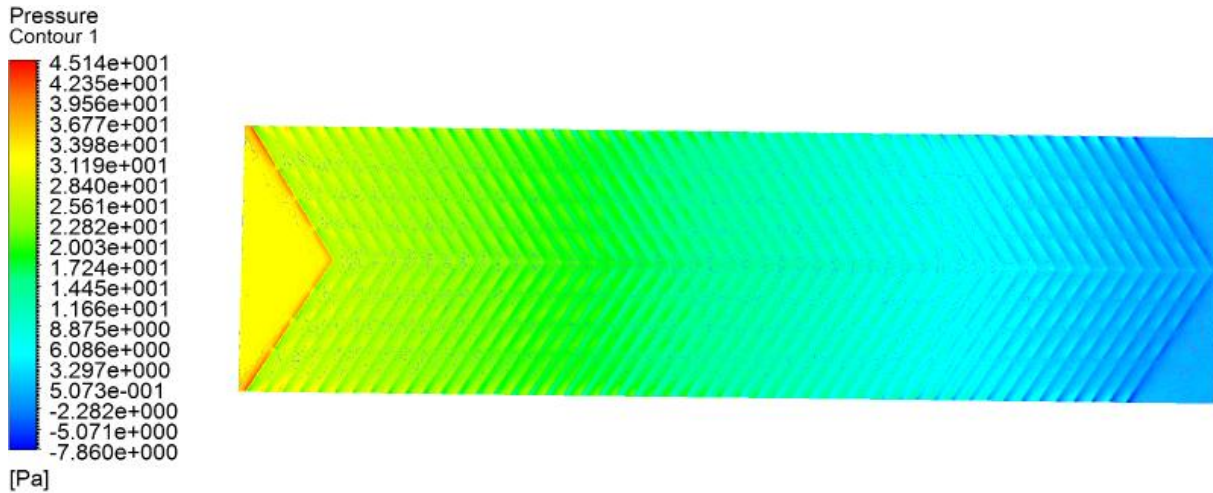
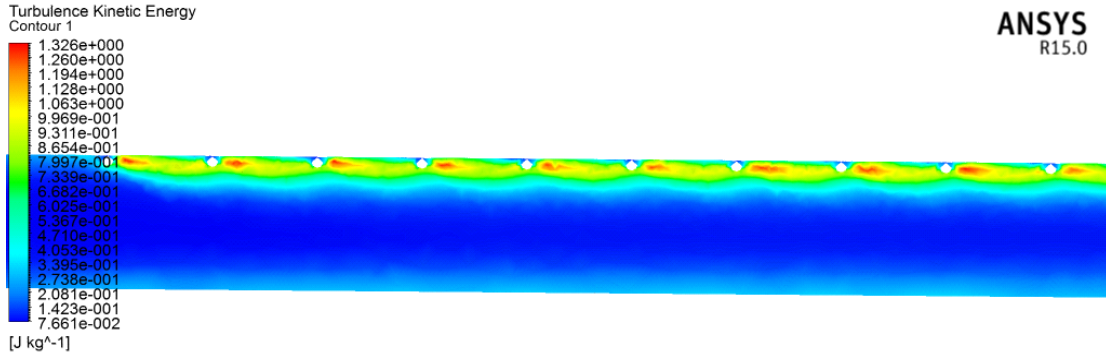


Fig.5. Contour of pressure at Reynolds number 15000

#### 4.2 Turbulence kinetic energy

The heat transfer phenomenon can be observed and described by the contour of turbulence kinetic energy. The contour plot of turbulence kinetic energy is shown in fig.6. Since the  $k-\epsilon$  models use  $\mu_t = \rho C_\mu k^2 / \epsilon$  as the turbulent viscosity, the high values of  $k$  in the flow field leads to high heat transfer predictions. It can be seen that near the wall the intensities of turbulence kinetic energy is reduced, whereas a high turbulence kinetic energy region is found between the adjacent ribs close to the main flow which results in the strong heat transfer enhancement.



**Fig.6. Contour of turbulence kinetic energy at Reynolds number 15000**

### 4.3 Velocity contour

Fig. 7. Shows the contour plot of velocity for Reynolds number of 15000 and stronger vortices can be seen because of the presence of rib roughness, which results in high heat transfer rate. The disturbance to laminar sub-layer is less for low Reynolds number, due to low velocity and it tends to low heat transfer rate. At high velocity, the disturbances are generated due to the roughness which minimizes the resistance due to laminar sub-layer.

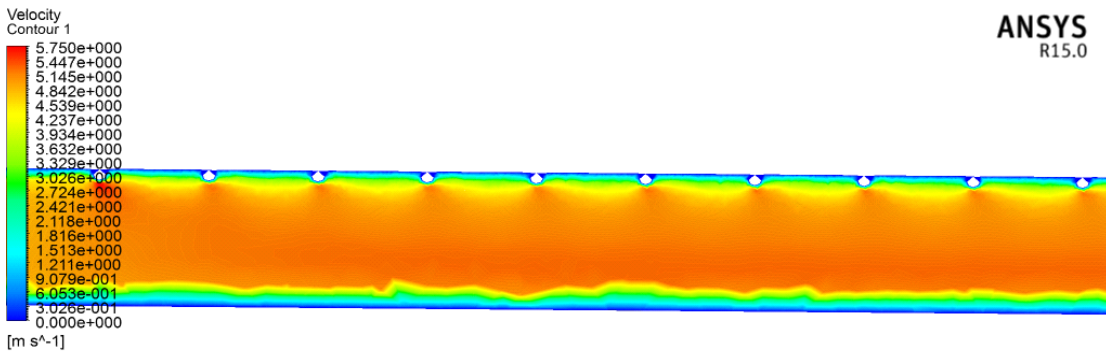


**Fig. 7. Contour plot of velocity for Reynolds number of 15000.**

### 4.4 Flow pattern

The flow pattern is shown in fig .8. It was clearly observed that the flow reattachment occurred in the downstream direction and the secondary flow appears in the region of spacing. The reattachment length is more over close the next rib. The secondary flow increases the turbulent intensity and it also contributes to stronger vortex and better fluid mixing.



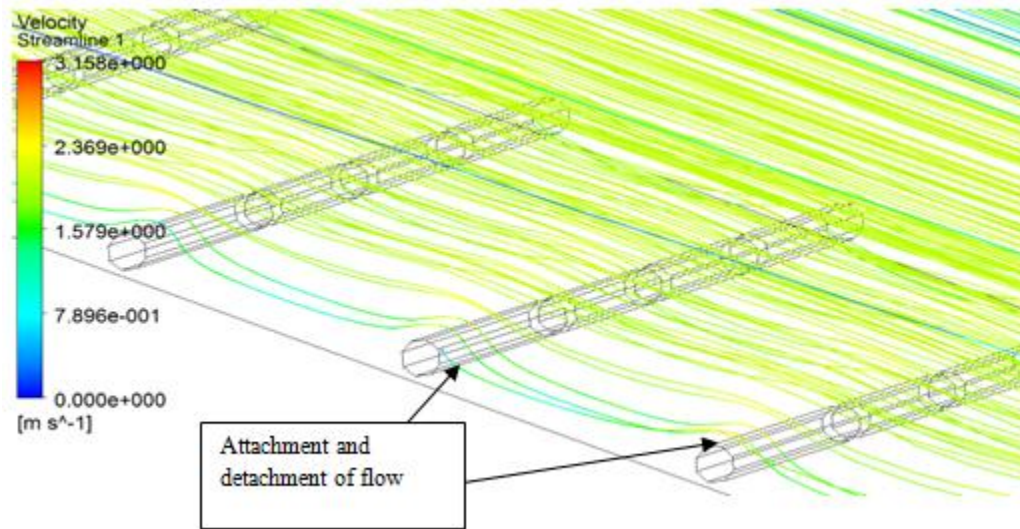


**Fig.8. Stream lines flow over the ribs.**

#### 4.5 Effect of rib pitch ( $P/e$ )

Fig.9. shows the effect of relative roughness pitch ( $P/e$ ) on friction factor and Nusselt number ( $Nu$ ) for different values of Reynolds number ( $Re$ ) and for fixed value of relative roughness height ( $e/D$ ) and angle of attack ( $\alpha$ ) of  $60^\circ$ . It is observed that the Nusselt number increases with the increase in ( $P/e$ ) and attains a maximum Nusselt number at  $P/e$  of 10. Further increase in the  $P/e$  reduces the Nusselt number as the number of reattachment points decreases with the increase in  $P/e$ . It has also seen that the friction factor increases with a decrease in relative roughness pitch. The maximum friction factor is attained at  $P/e=10$ .

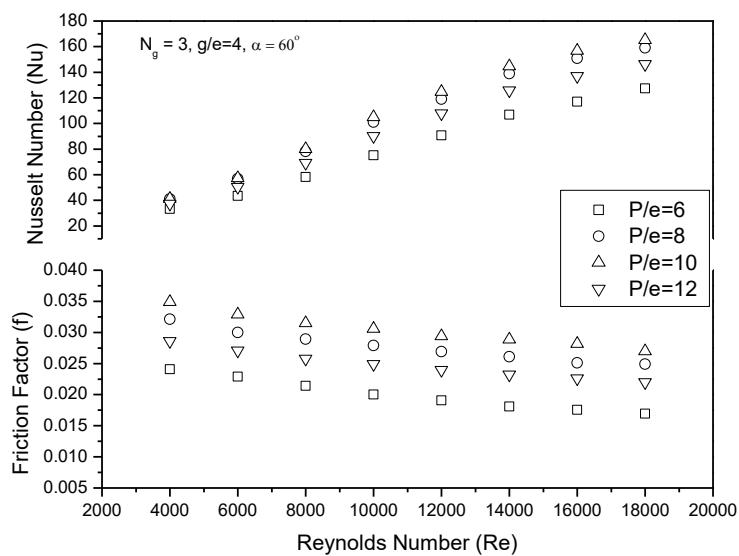


**Fig.9. Nusselt number and friction factor variation for different values of  $P/e$ .**

#### 4.6 Effect of angle of attack ( $\alpha$ )

Fig.10. shows the variation of Nusselt number and friction factor with Reynolds number at different values of angle of attack. The Nusselt number is found to be maximum for the angle of attack of  $60^\circ$  and at Reynolds number 18000, the least value of Nusselt number is obtained for the angle of attack of  $30^\circ$ . The friction factor is also maximum for the angle of attack of  $60^\circ$  and it further decreases with increase in Reynolds number. It is seen that Nusselt number and the friction factor corresponds to the maximum values at an angle of attack of  $60^\circ$ . It is due to flow separation in the secondary flow generated from the V-shaped ribs and the motion of vortices give up an optimum value of the angle of attack.

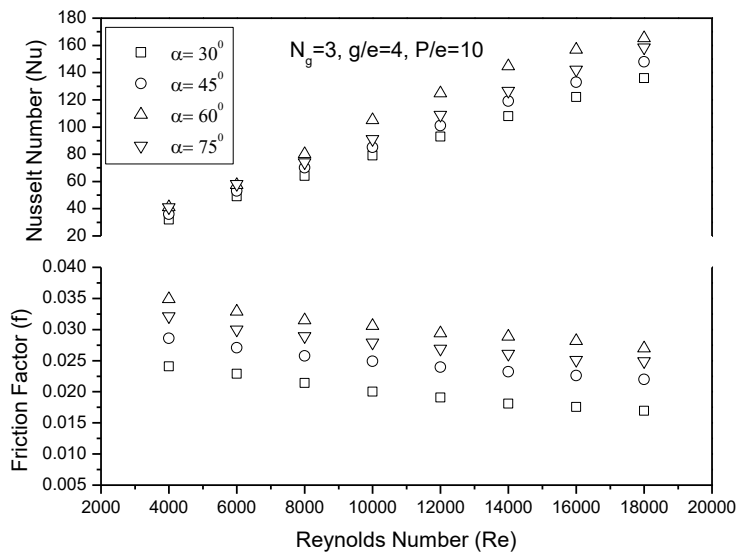


**Fig.10. Nusselt number and friction factor variation at different values of angle of attack**

#### 4.7 Thermo-hydraulic performance of an artificially roughened solar air heater

Fig.11.shows variation of thermo-hydraulic performance with Reynolds number at a different angle of attack it was observed that for the angle of attack  $60^\circ$  thermo-hydraulic performance was maximum attaining a value of 2.37. It can be concluded from the graph that thermo-hydraulic performance increases with Reynolds number up to 14000 and then starts decreasing. Fig.12 shows a variation of thermo-hydraulic performance with Reynolds number it can be seen that the hydraulic performance increases with increase in relative pitch and is maximum at  $P/e = 10$ .

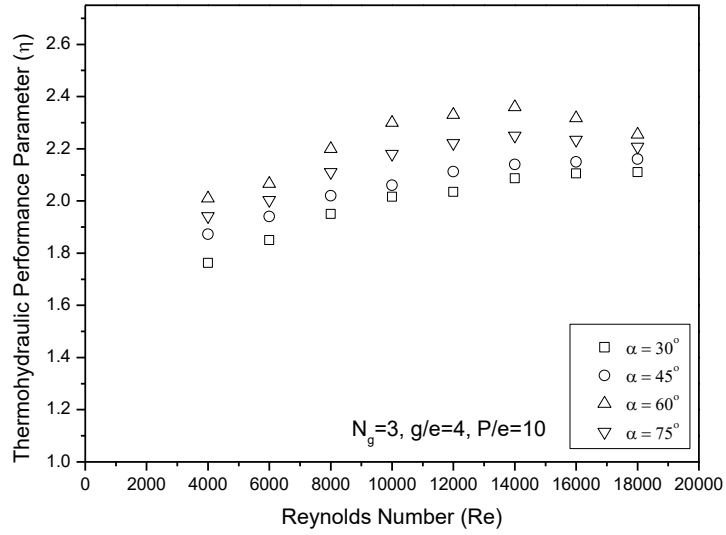


**Fig.11. Thermo hydraulic performance with Reynolds number at different angle of attack**

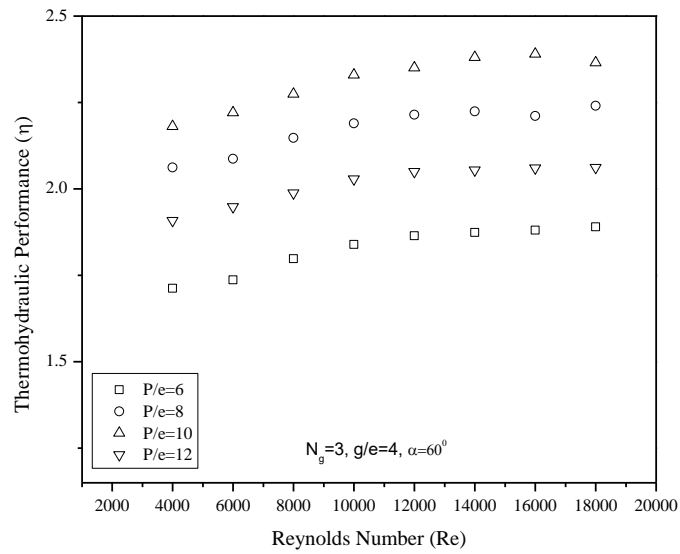


**Fig.12. Variation of thermo-hydraulic performance with Reynolds number**

## 5. Conclusions

The numerical study of heat transfer and fluid flows in the solar air heater duct enhanced with v-ribs in the absorber plate is carried out, with the aim to improve the overall thermo-hydraulic performance of the system. The major findings are summarized as follows:

1. The present study has been done by using Renormalization-group The RNG  $k-\epsilon$  turbulence model because it predicts very close results to that of experimental results as investigated by many researchers.
2. The average Nusselt number increases with the increase in Reynolds number. The average Nusselt number decreases with the increase in relative roughness pitch ( $P/e$ ) at constant relative roughness height ( $e/D$ ). The maximum Nusselt number is obtained at  $P/e=10$ .
3. The average friction factor decreases with the increase in Reynolds number. If the relative roughness pitch decreases the average values of friction factor increases for a fixed value of relative roughness height.
4. The results of CFD analysis are found to be in good agreement with the experimental results. So the present CFD module can be used for the analysis of the new geometries in solar air heater.
5. For an angle of attack  $30^\circ$  thermo-hydraulic performance was found to least and it further increases on increasing the angle of attack. At an angle of attack of  $60^\circ$  thermo-hydraulic performance was maximum.
6. Various CFD contours have been shown to visualize the effect of velocity, turbulence in kinetic energy, temperature and pressure at different Reynolds number.

### Nomenclature:

$h$	Convective heat-transfer coefficient ( $W/m^2K$ )
$f$	Friction factor of roughened duct
$g$	Gap size (m)
$D$	Hydraulic diameter of duct (m)
$k$	Thermal conductivity
$N_g$	Number of gaps
$Nu$	Nusselt number of roughened duct
$Nu_s$	Nusselt number of smooth duct
$P$	Pitch of the rib (m)
$e/D$	Relative roughness height
$P/e$	Relative roughness pitch
$g/e$	Relative gap width
$Re$	Reynolds number
$e$	Rib height (m)
$h$	Convective heat-transfer coefficient ( $W/m^2K$ )
$H$	Height of duct (m)

D	Hydraulic diameter of duct (m)
$\dot{m}$	Mass flow rate of air (kg/s)
U	Mean airflow velocity in the duct (m/s)

*Greek symbols*

$\alpha$	Angle of attack
$\eta$	Thermohydraulic performance parameter
v	Air flow velocity in y-direction (m/s)

## References

- [1] Singh S., Chander S., Saini J.S. Heat transfer and friction factor correlations of solar air heater ducts artificially roughened with discrete V-down ribs. *Energy*, 36 (2011). pp. 5053–5064.
- [2] Kumar A., Saini R.P, Saini J.S. Heat and fluid flow characteristics of roughened solar air heater ducts e a review. *Renewable Energy*, 47 (2012), pp. 77–94.
- [3] Chaube Alok., Sahoo PK, Solanki SC. Analysis of heat transfer augmentation and flow characteristics due to rib roughness over absorber plate of a solar air heater. *Renewable Energy*, 31 (2006), pp. 317–31.
- [4] A.S. Yadav, J.L. Bhagoria, A CFD-based heat transfer and fluid flow analysis of a solar air heater provided with circular transverse wire rib roughness on the absorber plate, *Energy*, 55 (2013), pp. 1127–1142.
- [5] Varun, R.P. Saini, S.K. Singal, Investigation of thermal performance of solar air heater having roughness elements as a combination of inclined and transverse ribs on absorber plate, *Renewable Energy*, 33 (2008), pp. 1398–1405.
- [6] Tanda G. Performance of solar air heater ducts with different types of ribs on the absorber plate. *Energy*, 36 (2011), pp. 6651–60.
- [7] Muluwork K.B. Investigations on fluid flow and heat transfer in roughened absorber solar heaters, Ph.D. dissertation (2000) IIT Roorkee.
- [8] Momin AME, Saini JS, Solanki SC. Heat transfer and friction in solar air heater duct with V-shaped rib roughness on absorber plate. *International Journal of Heat and Mass Transfer*, 45 (2002), pp. 3383–96.
- [9] Anil Kumar, Muneesh Sethi, Khushmeet Kumar, Sourabh Khurana and Abhilash Pathania "Computational Fluid Dynamics Based Analysis of Angled Rib Roughened Solar Air Heater Duct"*International Journal of Thermal Technologies*, 3 (2013) 2, pp. 43-47.
- [10] Anil Kumar, Man-Hoe Kim, " Effect of roughness width ratios in discrete multi V-rib with staggered rib roughness on overall thermal performance of solar air channel " *Solar Energy*, 119 (2015), pp. 399–414.
- [11] Sahu, MM.,Bhagoria,JL., "Augmentation of heat transfer coefficient by using 90° broken transverse ribs on absorber plate of solar air heater ". *Renewable Energy*, 30 (2005), pp. 2057–73.

- [12] Sharma AK, Thakur NS. CFD based fluid flow and heat transfer analysis of a v- shaped roughened surface solar air heater. *International Journal of Advanced Engineering Technology*, 4 (2012) 5, pp. 2115–21.
- [13] Maithani R., Saini, J.S., "Heat transfer and fluid flow behavior of a rectangular duct roughened with V-ribs with symmetrical gaps", *Int. J. Ambient Energy*, (2015), DOI:10.1080/01430750.1100681
- [14] A.S. Yadav, J.L. Bhagoria, A CFD based heat transfer and fluid flow analysis of a solar air heater provided with circular transverse wire rib roughness on the absorber plate, *Energy*, 55 (2013), pp. 1127–1142.
- [15] A. Kumar, R.P. Saini, J.S. Saini, Experimental investigation on heat transfer and fluid flow characteristics of air flow in a rectangular duct with Multi v-shaped rib with gap roughness on the heated plate, *Sol. Energy*, 86 (2012), pp. 1733–1749.